Intraband carrier dynamics in InAs/GaAs quantum dots stimulated by bound-tocontinuum excitation

Harada, Yukihiro
Maeda, Tsuyoshi
Kita, Takashi

(Citation)
Journal of Applied Physics,113:223511-223511

(Issue Date)
2013

(Resource Type)
journal article

(Version)
Version of Record

(URL)
https://hdl.handle.net/20.500.14094/90002577

Intraband carrier dynamics in InAs/GaAs quantum dots stimulated by bound-to-continuum excitation

Yukihiro Harada, Tsuyoshi Maeda, and Takashi Kita

Citation: Journal of Applied Physics **113**, 223511 (2013); doi: 10.1063/1.4810859
View online: http://dx.doi.org/10.1063/1.4810859
View Table of Contents: http://scitation.aip.org/content/aip/journal/jap/113/22?ver=pdfcov
Published by the AIP Publishing

Intraband carrier dynamics in InAs/GaAs quantum dots stimulated by bound-to-continuum excitation

Yukihiro Harada,[a] Tsuyoshi Maeda, and Takashi Kita
Department of Electrical and Electronic Engineering, Graduate School of Engineering, Kobe University, 1-1 Rokkodai, Nada, Kobe 657-8501, Japan

(Received 10 April 2013; accepted 28 May 2013; published online 14 June 2013)

We studied state-filling-dependent intraband carrier dynamics in InAs/GaAs self-assembled quantum dots using two-color photoexcitation spectroscopy. The photoluminescence (PL) intensity was observed to be dramatically reduced by selectively pumping carriers from the intermediate state to the continuum state located above the conduction band edge, and the PL-intensity reduction decreased with an increase in the continuous-wave excitation power. We analyzed the observed state-filling-dependent intraband carrier dynamics by detailed modeling of carrier excitation and relaxation processes in which the two-photon absorption for the interband transition, Pauli blocking, and saturable absorption for the intraband transition is considered. © *2013 AIP Publishing LLC*. [http://dx.doi.org/10.1063/1.4810859]

I. INTRODUCTION

Intraband transitions in self-assembled InAs/GaAs quantum dots (QDs) have attracted much attention for the realization of high-performance optical devices operating at near- to far-infrared (IR) wavelengths, such as mid-IR emitters,[1] IR photodetectors,[2–5] and intermediate-band solar cells.[6–8] The strength of the intraband absorption is an important quantity for determining device performance. The intraband absorption spectrum of QDs has been calculated by effective mass approximation.[9–12] Recently, Luque *et al.* reported that the intraband absorption coefficient for both the *bound-to-bound* and *bound-to-continuum* transitions is comparable to the interband absorption coefficient in QDs.[12]

On the other hand, the intraband absorption in InAs/GaAs QDs has been measured by photoinduced absorption spectroscopy[13,14] and time-resolved photoluminescence (PL) quenching measurements.[15,16] Besides, we recently succeeded in observing an enhancement of the *bound-to-continuum* intraband transition in InAs/GaAs QDs embedded in a photonic cavity by time-resolved PL quenching measurements.[17] By controlling the resonant wavelength of the photonic cavity, we can selectively improve the intraband transition. In the present paper, we report on the state-filling-dependent intraband carrier dynamics in InAs/GaAs quantum dots stimulated by *bound-to-continuum* excitation.

II. EXPERIMENT

InAs/GaAs self-assembled QDs embedded in a GaAs λ cavity that includes two GaAs/AlAs distributed Bragg reflector (DBR) mirrors were grown by solid-source molecular beam epitaxy. After thermally cleaning an undoped GaAs(001) substrate, a 500 nm GaAs buffer layer was grown at 550 °C. Then, the substrate temperature and the As_2 flux were set at 500 °C and 1.0×10^{-5} Torr, respectively. The nominal deposition rate of GaAs/AlAs DBR mirrors was 1.0 monolayer per second (ML/s). The periods of the top and bottom mirrors were 5 and 9, respectively. The resonance wavelength λ_c was chosen to be 1300 nm, and the measured Q value of this cavity was 77.[17] Thus, the cavity can selectively enhance the optical transition from the intermediate state to the continuum state located above the conduction band (CB) edge. QD layers were inserted into the cavity at the anti-node positions of the electromagnetic field to enhance the QD-light interaction.[17] Three InAs QD layers were prepared by the Stranski–Krastanov growth mode. The substrate temperature and the As_2 flux were set at 480 °C and 1.0×10^{-5} Torr, respectively, during the growth of the cavity layer. InAs QDs were formed by depositing a 2.4 ML of InAs with the nominal deposition rate of 0.04 ML/s. The thickness of the GaAs spacer layer between the QD layers was 50 nm. The average QD height was ~5 nm, and the base lengths were approximately 21 and 23 nm along [110] and [–110] crystal axes, respectively.[18,19] The QD density was $\sim 4 \times 10^{10}$ cm^{-2}. The 50-nm GaAs spacer layer is thick enough to separate each QD layer, and thus the electronic coupling between QDs stacked along the growth direction is negligible. Furthermore, we provided a reference sample with three InAs QD layers without the cavity structure. The QDs were grown under the same conditions.

Two-color photoexcitation spectroscopy was carried out at 4 K using a near-IR streak-camera system. A 659-nm continuous-wave (CW) laser was used to irradiate the sample to create carriers in the QD system. In the steady state, the carrier density of the intermediate state is limited by the radiative recombination rate. Then, the intermediate state was selectively excited by 1300-nm pulsed laser light. This pulsed light was generated by an optical parametric oscillator excited by a mode-locked Ti:sapphire pulse laser. The pulse duration was approximately 200 fs and a repetition rate was 80 MHz. The laser beam diameter of both the CW- and pulse-excitation lasers at the sample surface was 300 μm. In this study, we observed streak-camera images of the PL created by the CW laser light. Here, we consider the interband

[a]Electronic mail: y.harada@eedept.kobe-u.ac.jp.

transition between the intermediate state and the quantized hole state in QDs. The PL intensity changes according to a change in the carrier density of the intermediate state that is modulated by the ultrafast IR laser pulse excitation.

III. RESULTS AND DISCUSSION

Figure 1(a) shows a typical PL spectrum of the reference sample measured at 17 K. The CW-excitation power was 1 mW. The peak wavelength of the PL is approximately 1140 nm, which is shorter than the 1300 nm of the pulse excitation wavelength as indicated by the arrow. In the two-color photoexcitation spectroscopy performed at 4 K for the sample with the cavity, the laser pulses exciting the sample passes through the fundamental interband optical gap without being absorbed. However, the absorption edge of the intraband transition at 4 K is approximately 3000 nm, which is longer than the 1300 nm excitation pulsed laser light. Thus, the pulse excitation causes the *bound-to-continuum* intraband transition.

When the intermediate state is excited by laser pulses, the carrier density of the intermediate state decreases, thus reducing the radiative recombination. This will be observed by a change in the PL intensity. We successfully observed a very clear reduction in the PL intensity and the following temporal evolution.[17] A typical result obtained for the sample with the cavity is shown in Fig. 1(b). Here, we indicate the PL intensity integrated in the whole spectrum. The CW-excitation power was 1 mW, the pulse-excitation power was 125 mW, and the sample temperature was 4 K. The PL intensity abruptly decreases and shows a dip structure just after the pulse excitation. This is direct evidence of carrier excitation from the intermediate state and subsequent relaxation to the initial state. It is noted that this dip structure in the PL response is followed by a gain, which indicates that extra carriers should be generated by the pulse excitation. The gain signal also shows a relatively slow temporal response. The observed PL response results from the increased carrier density in GaAs created by both the *bound-to-continuum* intraband transition and the two-photon absorption (TPA) from the IR laser pulse excitation.[17] Similar results have been confirmed when using QDs without the cavity structure, though the PL intensity reduction becomes significant when using QDs with the cavity structure. When using the cavity structure, the signal amplitude increases by a factor of 8.[17]

Figure 2 shows the pulse-excitation power dependence of the maximum PL-intensity reduction for the sample with the cavity. Squares, circles, and triangles indicate the results for the CW-excitation powers of 0.25, 1.0, and 1.5 mW, respectively. The PL-intensity reduction strongly depends on the CW-excitation power; the low CW-excitation power considerably reduces the PL intensity at low pulse-excitation power. On the other hand, a dramatic difference is observed between CW-excitation powers of 1.0 and 1.5 mW. No obvious PL-intensity reduction was observed below the pulse-excitation power of 150 mW for the CW-excitation power of 1.5 mW. In order to understand the observed CW- and pulse-excitation power-dependent PL dynamics, we developed the phenomenological rate equations in Ref. 17 by taking into account the effect of the saturable absorption for the *bound-to-continuum* intraband transition.

Figure 3(a) shows a model for interpreting the observed results. The CW laser excites the valence band (VB) electrons to the CB at the rate G. The populated electron density in the CB is n_C. The excited electrons relax to the intermediate state

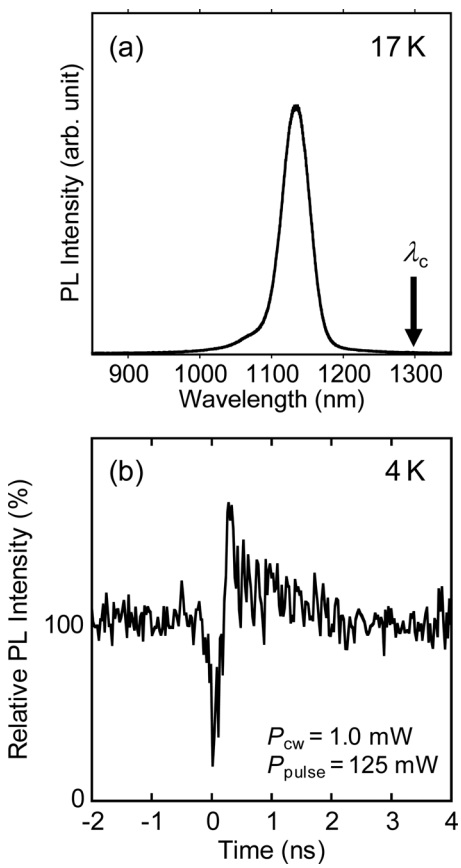

FIG. 1. (a) Typical PL spectrum of InAs/GaAs QDs measured at 17 K. The CW-excitation power was 1 mW. (b) Typical two-color excitation signal of InAs/GaAs QDs in cavity measured at 4 K. PL intensity was integrated in the whole spectrum. The CW-excitation power was 1 mW, and the pulse-excitation power was 125 mW.

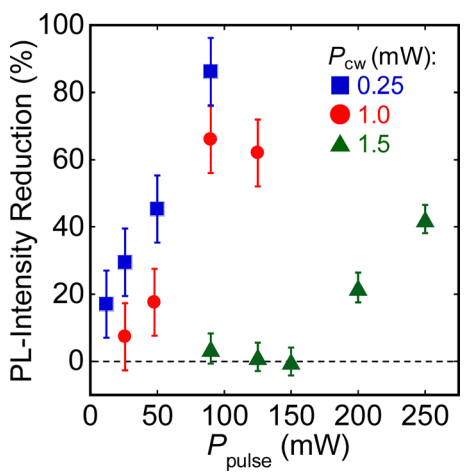

FIG. 2. Pulse-excitation power dependence of the maximum PL-intensity reduction for the sample with the cavity. Squares, circles, and triangles indicate the results for the CW-excitation powers of 0.25, 1.0, and 1.5 mW, respectively.

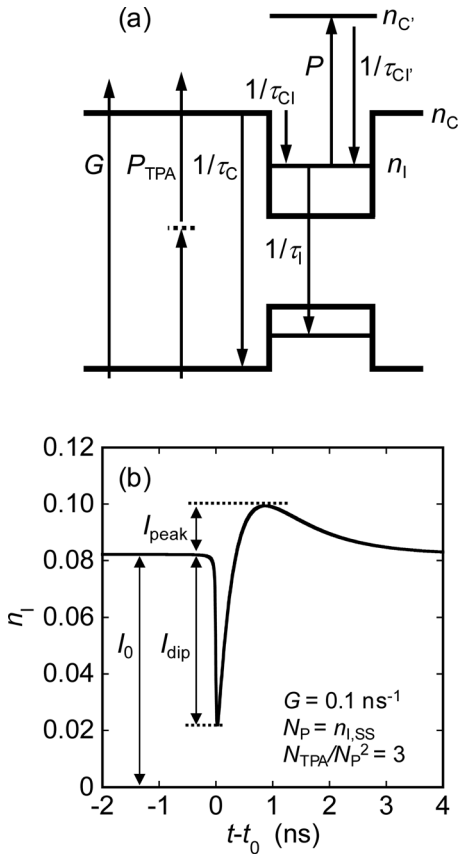

FIG. 3. (a) Three-level model for representing excitation and relaxation processes. (b) Typical calculated responses of PL intensity created by a pulse excitation at $G = 0.1\,\mathrm{ns}^{-1}$ and $N_{\mathrm{TPA}}/N_{\mathrm{P}}^2 = 3$. N_{P} is assumed to be equal to the steady-state value of n_{I}.

or the VB with time constants of τ_{CI} and τ_{C}, respectively. The electron density of the intermediate state is n_{I}. Electrons in the intermediate state recombine in radiative and nonradiative processes with a time constant of τ_{I}. The IR laser pulse excites the intermediate state electrons to the CB. The density of the electrons that are excited by the IR laser pulse in the CB is $n_{C'}$, which relaxes to the intermediate state with a time constant of $\tau_{C'I}$. Here, we neglected excitation from the GaAs CB edge to the excited states in the CB, because the excitation rate of such a spatially delocalized initial state is relatively very small. The excitation rate by the IR laser is expected to be proportional to the laser shape. The sech^2-shaped function was used to represent the excitation pulse shape at time t_0. The number of excited electrons per pulse is N_P. Using these parameters, the following phenomenological rate equations can be derived:[17]

$$\frac{\partial n_{\mathrm{C}}}{\partial t} = G - \frac{n_{\mathrm{C}}}{\tau_{\mathrm{CI}}}\left(1 - \frac{n_{\mathrm{I}}}{2}\right) - \frac{n_{\mathrm{C}}}{\tau_{\mathrm{C}}} + P_{\mathrm{TPA}},$$

$$\frac{\partial n_{\mathrm{C}'}}{\partial t} = -\frac{n_{\mathrm{C}'}}{\tau_{\mathrm{C'I}}}\left(1 - \frac{n_{\mathrm{I}}}{2}\right) + P,$$

$$\frac{\partial n_{\mathrm{I}}}{\partial t} = \frac{n_{\mathrm{C}}}{\tau_{\mathrm{CI}}}\left(1 - \frac{n_{\mathrm{I}}}{2}\right) + \frac{n_{\mathrm{C}'}}{\tau_{\mathrm{C'I}}}\left(1 - \frac{n_{\mathrm{I}}}{2}\right) - \frac{n_{\mathrm{I}}}{\tau_{\mathrm{I}}} - P,$$

$$P_{(\mathrm{TPA})} = \frac{N_{\mathrm{P(TPA)}}}{2\Delta}\,\mathrm{sech}^2\left(\frac{t - t_0}{\Delta}\right).$$

The third equation describes carrier density in the intermediate state, and the fourth one shows carrier densities generated in the intraband transition and TPA. P_{TPA} successfully interprets the gain feature that appeared just after the rapid reduction in n_{I}.[17] These equations include the Pauli blocking factor $1 - n_{\mathrm{I}}/2$ for the intermediate state. In the present study, the effect of saturable absorption on the *bound-to-continuum* intraband transition was taken into account when N_P is larger than the n_{I} at the steady state. The recombination time in the GaAs CB, τ_{C}, was assumed to be 3.3 ns, which corresponds to the radiative lifetime of free excitons in GaAs.[20] We estimated τ_{CI} and τ_{I} from the time-resolved PL of the interband transition. The obtained τ_{CI} and τ_{I} were 0.3 and 0.9 ns, respectively.[17] Using these values, we calculated the PL response according to the temporal dependence of n_{I} which is broadened by convolution with a Lorentzian with a full width at half maximum of 20 ps which is the resolution of our streak camera system.

Figure 3(b) shows a typical calculated response of PL intensity created by a pulse excitation at $G = 0.1\,\mathrm{ns}^{-1}$ and $N_{\mathrm{TPA}}/N_{\mathrm{P}}^2 = 3$. N_{P} is assumed to be equal to the steady-state value of $n_{\mathrm{I}}(n_{\mathrm{I,SS}})$. Here, I_0, I_{dip}, and I_{peak} represent the base, reduced, and increased signal intensities, respectively. The observed dip structure in the PL response followed by the gain shown in Fig. 1(b) is well reproduced by this calculation.[17]

Figure 4 summarizes the G and N_P dependence of the calculated response of PL intensity at the $N_{\mathrm{TPA}}/N_{\mathrm{P}}^2$ of 3. The CW-excitation power G is 0.01, 0.1, 1, and $10\,\mathrm{ns}^{-1}$. Here, the pulse-excitation power is proportional to $N_P + 2N_{\mathrm{TPA}}$, whereas the intraband transition rate is proportional to $n_{\mathrm{I,SS}}$. Therefore, the pulse-excitation power is proportional to $(N_P + 2N_{\mathrm{TPA}})/n_{\mathrm{I,SS}}$ when the incident photon number of the pulsed light is much larger than $N_P + 2N_{\mathrm{TPA}}$. Figures 4(a)–4(c) show the results for $(N_P + 2N_{\mathrm{TPA}})/n_{\mathrm{I,SS}}$ of 0.5, 1, and 1.5, respectively. Here, the intensity of the spectrum was normalized. The normalized factor for each signal calculated at different values of G is shown in Fig. 4(a). Both the dip and gain structures are very clear for G smaller than $1\,\mathrm{ns}^{-1}$. It is noted that the relative amplitude of the dip (I_{dip}/I_0) becomes small and the response becomes fast for all N_P with an increase in G. This is caused by rapid carrier relaxation from GaAs into QDs. On the other hand, the relative amplitude of the peak (I_{peak}/I_0) becomes large with an increase in N_P for the same G. In contrast, the gain signal also disappears with increasing G greater than $1\,\mathrm{ns}^{-1}$ due to Pauli blocking. When G is too large, the total number of carriers excited by CW excitation is much larger than that by the pulse excitation. Therefore, the relative amplitude of the signal caused by pulse excitation becomes small compared with the signal level created by CW excitation.

Figures 5(a) and 5(b) show the calculated pulse-excitation power dependence of the maximum PL-intensity reduction (I_{dip}/I_0) and gain (I_{peak}/I_0), respectively, at the $N_{\mathrm{TPA}}/N_{\mathrm{P}}^2$ of 3. The maximum PL-intensity reduction decreases with an increase in G, which results from the rapid carrier relaxation from GaAs into QDs as discussed in Fig. 4. On the other hand, a saturation of the maximum PL-intensity reduction is obvious with an increase in the pulse-excitation

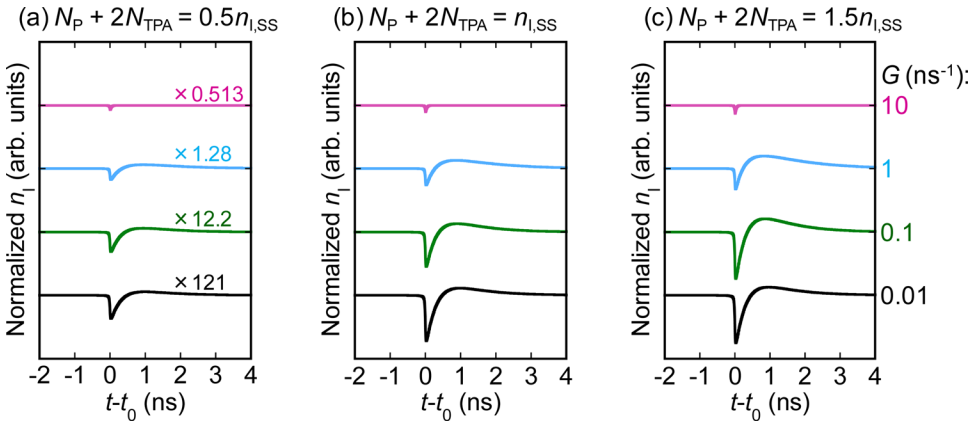

FIG. 4. G and N_P dependence of the calculated response of PL intensity at the N_{TPA}/N_P^2 of 3. (a)–(c) show the results for $(N_P + 2N_{TPA})/n_{I,SS}$ of 0.5, 1, and 1.5, respectively.

power when G is smaller than 0.1 ns^{-1}. This feature is caused by the saturable absorption for the *bound-to-continuum* intraband transition. However, the maximum PL-intensity gain shows a nonmonotonic dependence of the pulse-excitation power; the gain increases with increasing G below 0.3 ns^{-1}, whereas it decreases above 0.3 ns^{-1} due to Pauli blocking. Furthermore, a saturation of the maximum PL-intensity gain is observed as well as the reduction when the G is smaller than 0.1 ns^{-1}. We confirmed that these results are qualitatively independent of the N_{TPA}/N_P^2.

The calculated PL-intensity reduction gradually decreases with the increase in G at the $(N_P + 2N_{TPA})/n_{I,SS}$ of less than 1 as shown in Fig. 5(a), whereas the abrupt change in the experimental PL-intensity reduction was observed between the CW-excitation powers of 1.0 and 1.5 mW in Fig. 2. This discrepancy is considered to be caused by a low signal-to-noise ratio of the PL signal. Since the PL-intensity reduction decreases with the increase in G as shown in Figs. 4 and 5(a), the low signal-to-noise ratio is considered to cause the underestimation of the PL-intensity reduction with the increase in the CW-excitation power. However, the calculated pulse-excitation power dependence of the maximum PL-intensity reduction shown in Fig. 5(a) moderately reproduce the observed results in Fig. 2; the low CW-excitation power causes a significant reduction in the PL intensity at low pulse-excitation power, and the saturation of the maximum PL-intensity reduction is observed with an increase in the pulse-excitation power. Since a CW-excitation power of 1 mW corresponds to $G = 0.1$ ns^{-1}, the N_P/N_{TPA} is estimated to be approximately 4.0 at $N_{TPA}/N_P^2 = 3$ and 2.4 at $N_{TPA}/N_P^2 = 5$, when the PL-intensity reduction shows the maximum value. These values of N_P/N_{TPA} lead to the absorption coefficient of approximately 200 cm^{-1} for the *bound-to-continuum* transition. Here, the intermediate state was approximately 4% filled. Therefore, the absorption coefficient is estimated to be approximately 5×10^3 cm^{-1} in case the intermediate state is completely filled. According to the enhancement factor of 8 for the PL-intensity reduction in the cavity structure,[17] the absorption coefficient without the cavity structure can be roughly estimated to be approximately 600 cm^{-1} at the completely filled condition. This absorption coefficient moderately agrees with the value recently calculated by Luque *et al.*[12]

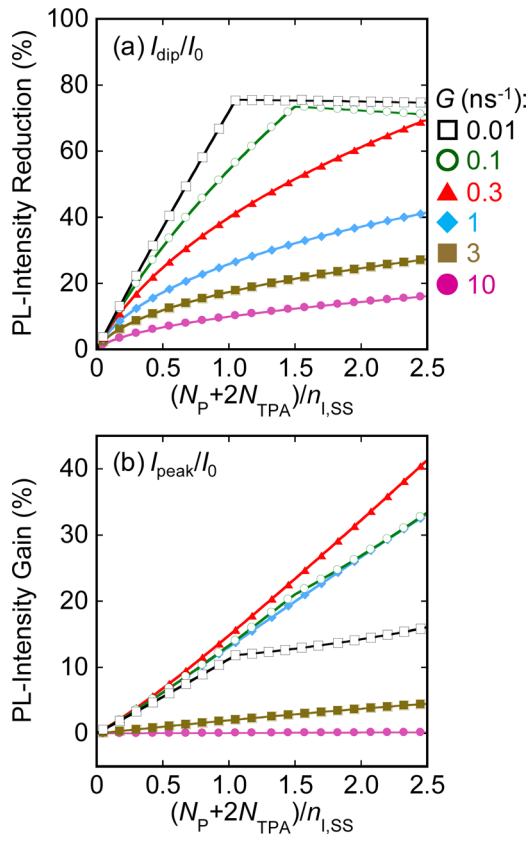

FIG. 5. Calculated pulse-excitation power dependence of the maximum PL-intensity (a) reduction and (b) gain at the N_{TPA}/N_P^2 of 3.

IV. CONCLUSIONS

Intraband carrier dynamics in InAs/GaAs self-assembled QDs embedded in a one-dimensional photonic cavity structure has been studied using two-color photoexcitation spectroscopy. The PL intensity was observed to be dramatically reduced by selectively pumping carriers from the intermediate state to the continuum state located above the CB edge, and the relative PL-intensity reduction decreased with an increase in the CW-excitation power. The intraband carrier dynamics has been analyzed by detailed modeling of carrier excitation and relaxation processes, which the TPA for the interband transition, Pauli blocking, and saturable absorption for the intraband transition are taken into account. The calculated results qualitatively

reproduced the observed state-filling-dependent intraband carrier dynamics.

ACKNOWLEDGMENTS

This work has been partially supported by the Scientific Research Grants-in-Aid from Ministry of Education, Culture, Sports, Science and Technology (MEXT), Japan, and the European Commission and New Energy and Industrial Technology Development Organization (NEDO) through the funding of a new generation of concentrator photovoltaic cells, modules, and systems (NGCPV) EUROPE-JAPAN.

[1]D. Wasserman, T. Ribaudo, S. A. Lyon, S. K. Lyo, and E. A. Shaner, Appl. Phys. Lett. **94**, 061101 (2009).
[2]P. Martyniuk and A. Rogalski, Prog. Quantum Electron. **32**, 89 (2008).
[3]A. Rogalski, J. Phys.: Conf. Ser. **146**, 012030 (2009).
[4]A. D. Stiff-Roberts, J. Nanophoton. **3**, 031607 (2009).
[5]A. V. Barve, S. J. Lee, S. K. Noh, and S. Krishna, Laser Photon. Rev. **4**, 738 (2010).
[6]A. Luque, A. Martí, N. López, E. Antolín, E. Cánovas, C. Stanley, C. Farmer, L. J. Caballero, L. Cuadra, and J. L. Balenzategui, Appl. Phys. Lett. **87**, 083505 (2005).
[7]A. Martí, E. Antolín, C. R. Stanley, C. D. Farmer, N. López, P. Díaz, E. Cánovas, P. G. Linares, and A. Luque, Phys. Rev. Lett. **97**, 247701 (2006).
[8]Y. Okada, T. Morioka, K. Yoshida, R. Oshima, Y. Shoji, T. Inoue, and T. Kita, J. Appl. Phys. **109**, 024301 (2011).
[9]X. Jiang, S. S. Li, and M. Z. Tidrow, Physica E **5**, 27 (1999).
[10]V. G. Stoleru and E. Towe, Appl. Phys. Lett. **83**, 5026 (2003).
[11]B. H. Hong, S. I. Rybchenko, I. E. Itskevich, S. K. Haywood, C. H. Tan, P. Vines, and M. Hugues, J. Appl. Phys. **111**, 033713 (2012).
[12]A. Luque, A. Martí, A. Mellor, D. F. Marrón, I. Tobías, and E. Antolín, Prog. Photovolt: Res. Appl. **21**, 658 (2013).
[13]S. Sauvage, P. Boucaud, F. H. Julien, J.-M. Gérard, and V. Thierry-Mieg, Appl. Phys. Lett. **71**, 2785 (1997).
[14]S. Sauvage, P. Boucaud, J.-M. Gérard, and V. Thierry-Mieg, Phys. Rev. B **58**, 10562 (1998).
[15]B. N. Murdin, A. R. Hollingworth, J. A. Barker, D. G. Clarke, P. C. Findlay, C. R. Pidgeon, J.-P. R. Wells, I. V. Bradley, S. Malik, and R. Murray, Phys. Rev. B **62**, R7755 (2000).
[16]J. Bhattacharyya, S. Zybell, S. Winnerl, M. Helm, M. Hopkinson, L. R. Wilson, and H. Schneider, Appl. Phys. Lett. **100**, 152101 (2012).
[17]T. Kita, T. Maeda, and Y. Harada, Phys. Rev. B **86**, 035301 (2012).
[18]T. Kita, T. Inoue, O. Wada, M. Konno, T. Yaguchi, and T. Kamino, Appl. Phys. Lett. **90**, 041911 (2007).
[19]T. Inoue, T. Kita, O. Wada, M. Konno, T. Yaguchi, and T. Kamino, Appl. Phys. Lett. **92**, 031902 (2008).
[20]G. W. p't Hooft, W. A. J. A. van der Poel, L. W. Molenkamp, and C. T. Foxon, Phys. Rev. B **35**, 8281 (1987).